Review of MRI-based measurements of pulse wave velocity: a biomarker of arterial stiffness

Andrew L. Wentland[1,2], **Thomas M. Grist**[1,2], **Oliver Wieben**[1,2]

[1]Department of Medical Physics, [2]Department of Radiology, University of Wisconsin School of Medicine and Public Health,1111 Highland Avenue, Madison, WI 53705-2275, USA

Correspondence to: Oliver Wieben, PhD. University of Wisconsin School of Medicine & Public Health, Department of Medical Physics, 1111 Highland Avenue, Madison, WI 53705-2275, USA. Email: owieben@wisc.edu.

Abstract: Atherosclerosis is the leading cause of cardiovascular disease (CVD) in the Western world. In the early development of atherosclerosis, vessel walls remodel outwardly such that the vessel luminal diameter is minimally affected by early plaque development. Only in the late stages of the disease does the vessel lumen begin to narrow—leading to stenoses. As a result, angiographic techniques are not useful for diagnosing early atherosclerosis. Given the absence of stenoses in the early stages of atherosclerosis, CVD remains subclinical for decades. Thus, methods of diagnosing atherosclerosis early in the disease process are needed so that affected patients can receive the necessary interventions to prevent further disease progression. Pulse wave velocity (PWV) is a biomarker directly related to vessel stiffness that has the potential to provide information on early atherosclerotic disease burden. A number of clinical methods are available for evaluating global PWV, including applanation tonometry and ultrasound. However, these methods only provide a gross global measurement of PWV—from the carotid to femoral arteries—and may mitigate regional stiffness within the vasculature. Additionally, the distance measurements used in the PWV calculation with these methods can be highly inaccurate. Faster and more robust magnetic resonance imaging (MRI) sequences have facilitated increased interest in MRI-based PWV measurements. This review provides an overview of the state-of-the-art in MRI-based PWV measurements. In addition, both gold standard and clinical standard methods of computing PWV are discussed.

Keywords: Pulse wave velocity (PWV); arterial stiffness; atherosclerosis; magnetic resonance imaging (MRI); velocity mapping

Introduction

Atherosclerosis is defined as the development of plaques, otherwise known as thickening of the arterial vessel wall, due to the accumulation of cholesterol, fibrous tissue, calcification, and hemorrhage. A number of complications may arise from atherosclerotic plaques; for example, rupture of a plaque may lead to thrombosis, total vessel occlusion, stenoses, and embolisms. Furthermore, plaques weaken the underlying vessel wall media and may lead to the development of an aneurysm. Due to these complications, atherosclerosis is the leading cause of cardiovascular disease (CVD) in the Western world.

In terms of epidemiology, atherosclerosis begins in childhood and remains subclinical for decades. Studies have demonstrated that all individuals between the ages of 15 and 34 years have some degree of aortic fatty streaks (1), which are early forms of atherosclerotic plaques. However, there is a paucity of individuals who display symptoms in this age group. Herein is the problem with the diagnosis of atherosclerosis: typically atherosclerotic-induced CVD does not manifest clinically until middle age—when luminal changes can be observed with medical imaging. A diagnostic test, or biomarker, that is more sensitive to the development
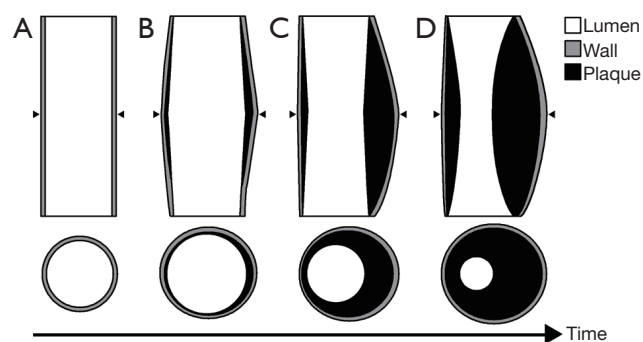
Figure 1 Glagov phenomenon showing plaque development over time in vessel cross-sections and along the length of the vessel. Compared to a normal vessel (A), early plaque development (B) causes outward remodeling of the vessel wall, which leads to either no change in vessel diameter or slight dilatation. Over time the compensatory dilatation of the vessel fails and the plaque begins to encroach upon the vessel lumen (C,D). Arrow heads identify the region from where the cross-sectional depictions are taken from the length-wise view of the vessels.

of atherosclerosis would be greatly useful for detecting disease in its early stages of development, such that lifestyle changes and medical therapy could be used to intervene and hinder disease progression.

Measurement of arterial stiffness has great potential to fill this void as increasing vessel wall stiffness—due to age and atherosclerosis—occurs long before luminal changes occur. Pulse wave velocity (PWV; also known as flow wave velocity) has emerged as a primary method to assess arterial stiffness; PWV is often measured with tonometry because of its relative ease of use and the large body of evidence regarding the association between PWV and CVD (2). PWV is defined as the rate at which the systolic bolus of blood, pumped from the heart, traverses the vasculature. Mathematically PWV is computed via the Moens-Korteweg equation Eq. [1]:

$$PWV = \sqrt{\frac{E \cdot h}{2r\rho}} \qquad [1]$$

where E is the elastic modulus of the vessel, h is vessel wall thickness, r is the vessel radius, and ρ is the blood density.

As atherosclerosis progresses vessel wall thickness (h) increases and vessel radius (r) decreases. These changes in vessel wall thickness and radius both serve to increase PWV as atherosclerosis develops Eq. [1]. PWV is potentially a very strong early biomarker of atherosclerosis, given that arterial stiffness first increases without changes in vascular geometry—via the Glagov phenomenon—

due to outward remodeling of atherosclerotic plaques (3) (*Figure 1*). In other words, the Glagov phenomenon describes a model in which early plaques grow outwardly into the vessel wall via a compensatory mechanism that preserves the luminal area of a vessel (*Figure 1B*). Because of the Glagov phenomenon, the vessel luminal diameter does not decrease in early atherosclerosis and therefore, early changes in arterial stiffness are not reflected on angiographic imaging, which only shows the preserved vessel lumen but not the diseased vessel wall. Only in late stages of atherosclerosis does the compensatory mechanism fail to overcome the tendency for plaques to narrow the vessel lumen (*Figure 1C,D*). Thus, late-stage atherosclerosis is apparent on angiographic images as a stenosis. As such, PWV may increase, and therefore detect the presence of atherosclerosis, earlier than the ability of angiography to detect stenoses and irregularities in the vasculature secondary to atherosclerosis.

A range of reference values for PWV have been reported in the literature. A large multi-center study in ~17,000 patients measured carotid-femoral PWV with tonometry and reported normal PWV values as ~6 m/s in healthy individuals younger than 30 years and up to ~10 m/s in individuals >70 years, independent of blood pressure (2). PWV increases further with hypertension and therefore affects PWV independently of age. An MR-based PWV study in 71 subjects found a mean aortic PWV of 3.6 m/s (4). The difference between these MR-based PWV measurements and the multi-center study of carotid-femoral PWV measurements is likely multifactorial; the difference could be caused by the lower temporal resolution of MR and/or the more focal nature of the MR-based measurements of the aorta instead of the more global carotid-femoral PWV measurements. Furthermore, the distance measurements used to compute PWV with tonometry are much less accurate than the distance measurements used in MR-based PWV measurements.

The computation of PWV with MRI was first discussed in 1989 (5). Renewed interest facilitated by faster and more robust MR imaging sequences has led to a recent rapid increase in reported studies with MRI-based PWV measurements. The purpose of this review is to summarize and synthesize the state-of-the-art in MRI-based PWV measurements. In addition, both gold standard and clinical standard methods of computing PWV will be reviewed briefly.

The differences between gold standard, clinical standard, and MRI-based measurements must be understood in the
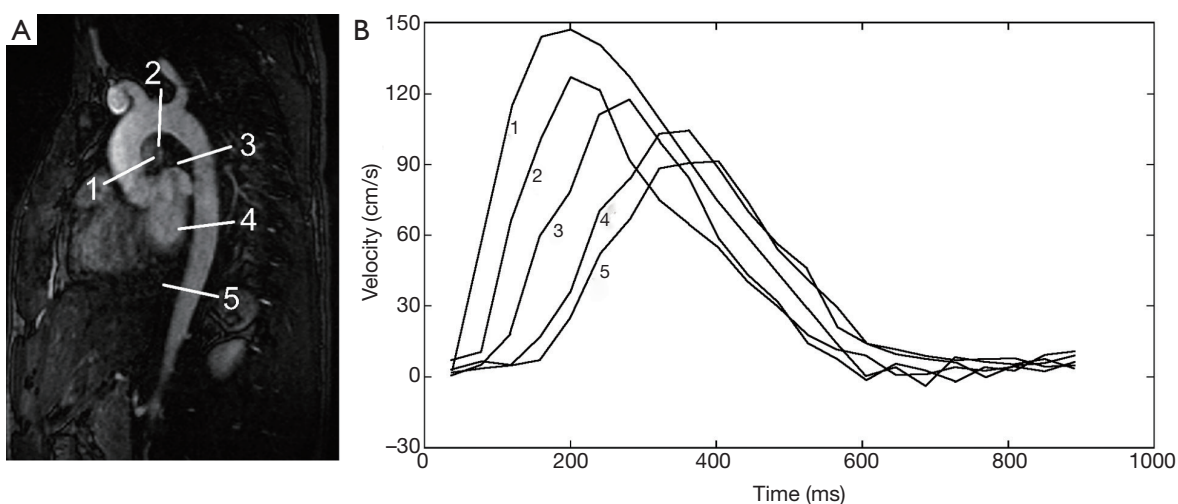
Figure 2 This double oblique view of the thoracic aorta from a magnetic resonance angiogram (MRA) (A) is used to show five slices from which aortic mean velocity waveforms are derived from a flow sensitive MR imaging sequence. (B) From the five velocity waveforms a temporal shift can be appreciated as the aorta is traversed. This shift can be used to compute the pulse wave velocity either regionally, for example from any two of these waveforms, or globally, using all of the waveforms. Note that maximum velocity decreases progressively at downstream slice locations; maximum velocity decreases for a number of reasons, including resistance to flow and loss of flow volume from vessels branching from the aorta. The 5 flow waveforms in (B) are derived from the 5 slices in (A).

context of global versus regional PWV measurements (*Figure 2*). The pulse wave can be understood as a wave superimposed on the flow/pressure waveform of the blood. This superimposed pulse wave accelerates and decelerates as it traverses distally in the vasculature relative to the stiffness of the vessel in a given vascular segment. With some of the methods described below, PWV is evaluated regionally in a small area of the vasculature [for example, computing PWV from the temporal shift between two subsequent velocity waveforms (*Figure 2B*)]. As a result, this PWV measurement is subject to sampling error, such that the area of evaluation could be in a region of stiffness, giving an elevated PWV, or the area of evaluation could be in an area of less stiffness, giving a lower PWV. If a vessel is heterogeneous in stiffness, a PWV measurement could be erroneous depending on the area selected for evaluating PWV. Some methods of computing PWV, including applanation tonometry, Doppler ultrasound and some MRI-based methods, evaluate PWV globally over a very large region of the vasculature [for example, computing PWV from the temporal shift amongst a series of velocity waveforms (*Figure 2B*)]. While global PWV measurements are minimally prone to sampling bias, areas of stiffness and elevated PWV will be averaged with normal areas of the vasculature. This averaging suppresses differences between individuals with a healthy vasculature

and individuals with sporadic areas of stiffness.

Gold standard measurements of pulse wave velocity

The gold standard of measuring PWV is via the use of flow meters or catheter-based pressure probes. Both pressure and flow waveforms within the vasculature can be used to detect the superimposed pulse wave. While these methods provide highly accurate measurements of PWV, the invasiveness involved in placing them intravascularly limits their use to animal studies or to patients otherwise undergoing cardiac catheterization.

Fiber optic probes can be used to measure pressure waveforms. Simultaneous data collection from two probes with a known distance between them are needed to measure PWV, such that the temporal shift between the two pressure waveforms can be used to compute PWV in the region between the tips of the two probes. Fiber optic probes use a Fabry-Perot interferometer configuration (6) and transmit pressure via a microelectromechanical system (MEMS), which houses a diaphragm that deflects in proportion to the amount of strain imparted on it. The pressure sensors contain temperature and pressure resistors. The pressure resistor is a strain gauge attached to a membrane that

deforms under pressure; the measurements are corrected via measurements with the temperature resistor. The outer diameter of these pressure probes is often less than 0.5 mm, which minimizes flow disturbances created by their presence within the vasculature. The pressure probes can be inserted with minimal invasiveness via an arterial cutdown.

PWV also can be measured with transit-time ultrasound flow meters (7). These flow meters are placed perivascularly and use an ultrasonic wave to measure flow. Within a given flow meter one ultrasonic wave is transmitted with the direction of flow and another wave is transmitted against the direction of flow. The difference in transit time between the upstream and downstream ultrasonic waves is directly proportional to the velocity of blood within a vessel. Regional PWV could be computed by noting the temporal shift between the flow waveforms of two ultrasonic flow meters separated by a known distance. This distance would need to be measured *in vivo* with a measuring tape after the flow meters are placed surgically. It may be difficult to measure accurately the separation distance, particularly if the distance between the two flow meters is large and the vessel is tortuous. The greater invasiveness needed to place the ultrasound flow meters perivascularly is a disadvantage of this method relative to the pressure probes.

Both the pressure probes and the ultrasonic flow meters provide a number of advantages that allow for highly accurate PWV measurements. The pressure probes have a high sampling rate, on the order of 100-2,000 Hz. While the two probes can be separated by a substantial distance for global PWV measurements, the high temporal resolution of these probes allows for the assessment of regional PWV. For example, if a subject's PWV is on the order of 10 m/s, and the sampling rate is 1,000 Hz, the two probes need to be separated by as little as 1 cm. Ultrasonic flow meters provide yet higher sampling rates, on the order of >1 MHz. There is effectively no minimum separation distance needed between two ultrasonic flow meters for computing PWV. Another advantage of the high temporal resolution provided by the pressure probes and ultrasonic flow meters is that pressure and flow waveforms are measured in real-time, and thus numerous cardiac cycles can be obtained in a few seconds. A PWV measurement can be obtained for every cardiac cycle, and thus averaged over all cardiac cycles, to account for any variability in PWV. A final advantage of both the fiber optic pressure probes and ultrasonic flow meters is that they can be made MR-compatible; these methods therefore allow for the direct validation of MRI-based PWV measurements.

The above methods provide high temporal resolution such that the shape of the pressure or velocity/flow waveform can be accurately depicted. On the other hand, sampling at lower temporal resolution can substantially change the shape of the waveform (*Figure 3*). As discussed below, PWV is computed from MR data using various characteristics of the waveform, such as the peak and foot of the waveform. As the temporal distance between sampling points becomes greater, the discretization error increases and there is a greater likelihood that these waveform characteristics will be misrepresented, leading to inaccurate PWV measurements.

Clinical methods of evaluating atherosclerotic disease

PWV is measured clinically with applanation tonometry (8,9) and Doppler ultrasound (9,10). In applanation tonometry, a tonometer is placed on the skin over both the carotid and femoral arteries. A pressure waveform is recorded from each location. The temporal shift between the carotid and femoral pressure waveforms is computed as the transit time, which predominantly uses the time-to-foot method, as described below. The distance measurement between these two vascular locations is calculated with a tape measure in either of two ways: (I) measuring the direct distance between the carotid and femoral arteries, or (II) taking the difference between the distance from the sternal notch to the femoral artery and the sternal notch to the carotid artery. This distance is divided by the transit time to compute PWV. The computation of PWV with Doppler ultrasound is identical to applanation tonometry, with the exception that ultrasound transducers are used instead of tonometers.

PWV with applanation tonometry and Doppler ultrasound have a number of benefits, including low cost, noninvasiveness, and lack of ionizing radiation. However, the distance measurement used in applanation tonometry and Doppler ultrasound can cause errors of up to 30% for the measurement of PWV (2,11,12). Equations to correct for inaccuracies in these distance measurements have been reported (13,14). Another problem with these techniques is that the method for measuring distance between the carotid and femoral arteries is not standardized and can lead to variations in the path-length used for PWV measurements (15-17). Variations in PWV between measurement centers are in part due to differences in the method of distance measurements. Also, obesity is a cause of operator bias in PWV measurements with applanation tonometry (18-20).
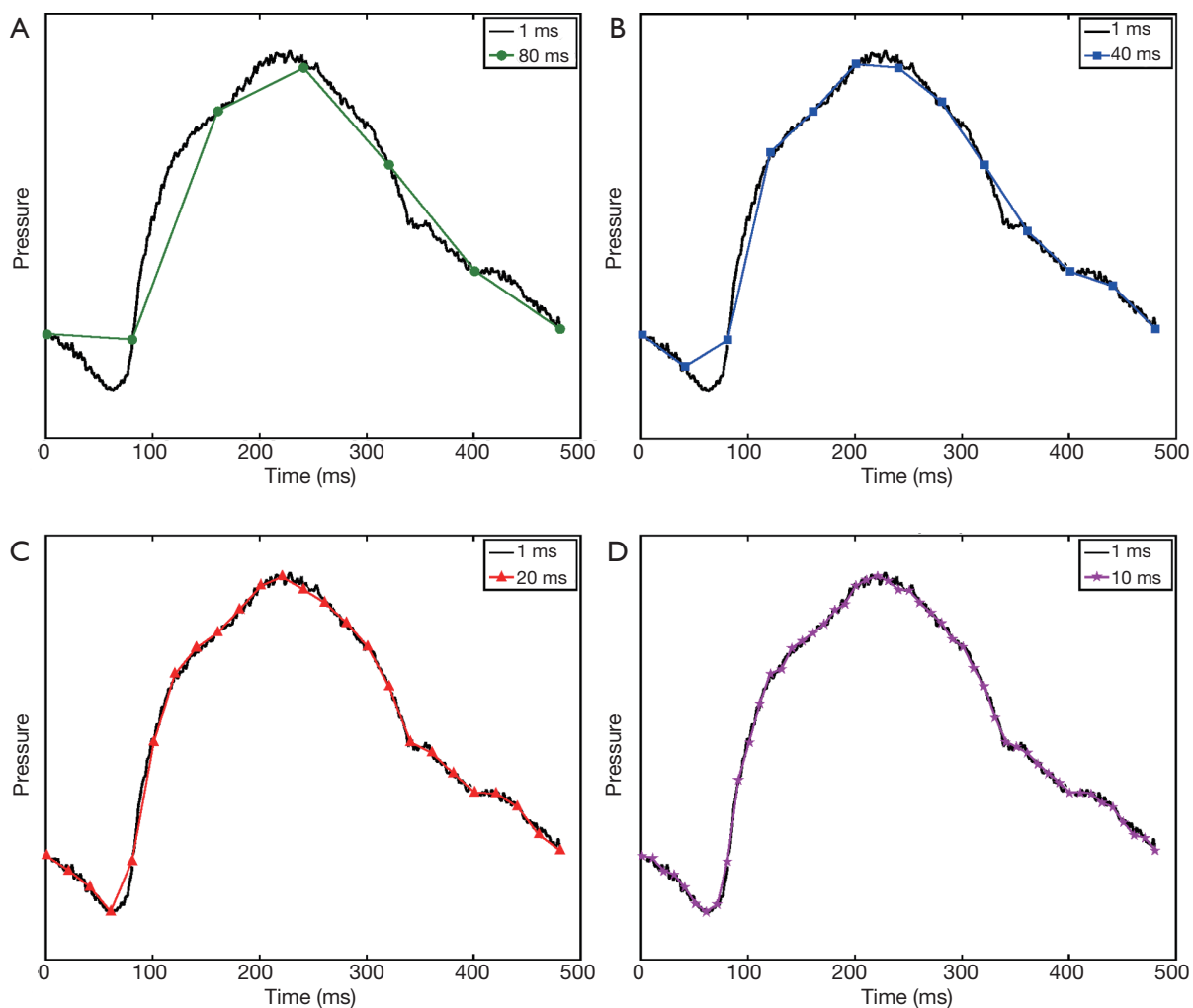
Figure 3 Sampling an aortic pressure waveform at 80 ms (A), 40 ms (B), 20 ms (C), and 10 ms (D) as compared to sampling at 1 ms. These high temporal resolution 1 ms data were acquired in the aorta of a pig with a fiber optic intravascular pressure sensor. For (A), (B), and (C) the waveform was downsampled to demonstrate that the shape of the waveform is highly dependent on adequate sampling of the data.

While applanation tonometry and Doppler ultrasound provide a global measurement of PWV, it should be noted that a recent ultrasound study was able to evaluate PWV regionally within the carotid artery (21). This regional measurement was made feasible by the high temporal resolution of ultrasound and the ability to measure distance within the beam imaging width.

Carotid intimal media thickness (CIMT) measurements are an alternative method of evaluating arterial stiffness (22). CIMT measurements are relatively easy to obtain, especially compared to the computation of PWV. However, they may also be user dependent and intimal thickening can occur in the absence of atherosclerosis (23). Also, ultrasound-based CIMT measurements have not demonstrated any predictive benefits to the Framingham Risk Score (FRS) (24), which is the standard method of assessing a patient's risk of a cardiovascular event based on patient risk factors. In comparison, one initial study has demonstrated that PWV measurements do indeed improve the predictive accuracy of the FRS (25).

Analysis methods for computing pulse wave velocity

There is a temporal shift, Δt, in the flow waveforms as the vasculature is traversed (*Figure 2B*). This temporal shift
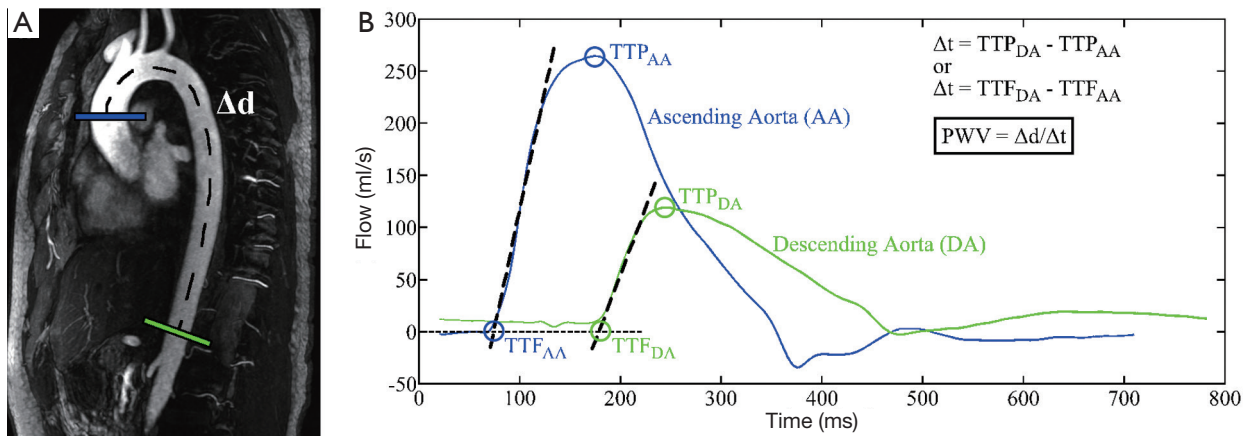
Figure 4 Double oblique view of the thoracic aorta from an MR angiogram (A) with representative planes in the ascending and descending thoracic aorta. Flow waveforms (B) from the two planes are shown with the time-to-foot (TTF) and time-to-peak (TTP) algorithms. The best fit linear lines along the upstroke were used to identify the feet of the waveforms. Please note that the two planes shown in (A) are used to represent the two waveforms shown in (B).

is related to the stiffness of the vessel, and the smaller the shift is, the greater the stiffness and the higher the PWV. The computation of PWV depends on analyzing various waveform characteristics to quantify the temporal shift from one waveform to another.

In *Figure 4* there are two planes highlighted to derive flow waveforms. The accurate measurement of the distance between the two planes, Δd, is important for the measurement of PWV; this distance (vessel path length) can be computed by measuring along the length of the vessel in the image. The simplest method of computing PWV is via the time-to-peak (TTP) method (*Figure 4*). With the TTP method the time point associated with the peak of the waveform is determined. The temporal shift, Δt, between two waveforms is therefore found by taking the difference between the two time points associated with the peaks of the two waveforms. Therefrom, the PWV is computed by dividing the distance between the two planes, Δd, by the temporal shift, Δt, such that $PWV=\Delta d/\Delta t$. The TTP method is highly prone to error given that the temporal shift is computed from a single data point from the flow waveforms; as a result, the TTP method is subject to sampling error such that the true peak of the waveform will often be missed (*Figure 3*). As a result, the PWV may be miscalculated.

More reliable methods of computing PWV use multiple points from the flow waveforms to mitigate sampling error. The time-to-foot (TTF) method is one such method that uses several time points (*Figure 4*) (26-29). This method

uses a linear best fit to data points along the upstroke of the flow waveform; oftentimes data points that are between 20% and 80% of the maximum are used for the best fit. The TTF is identified as the point of intersection between the linear fit of the upstroke with either the horizontal axis or another line fitted to the data points of the waveform prior to the upstroke. Again, the temporal shift, Δt, is computed by taking the difference between the TTFs of two flow waveforms; the PWV can then be computed as before. Time-to-upstroke (TTU) is a method that also uses the upstroke of the flow waveform. This method uses derivatives to find the greatest rate of change along the upstroke. While this method is less subject to sampling error than the TTP method, it is more susceptible to noise that may lead to large rate changes in the derivative. Another method that uses information in the upstroke fits a sigmoid to the upstroke and searches for the temporal shift in the maximum curvature between two flow waveforms (30,31).

Cross-correlation (XCorr) is a method of computing PWV that uses the entire flow waveform (32). In the XCorr operation a downstream flow waveform is incrementally shifted in time relative to the upstream waveform, which produces a correlation plot. The time shift needed to produce the greatest correlation is used as Δt in the computation of PWV. The XCorr method rivals the TTF method and may in fact be more repeatable (32). A study by Ibrahim *et al.* found the TTF method to be more reliable than the XCorr method (33).

www.thecdt.org   *Cardiovasc Diagn Ther* 2014;4(2):193-206
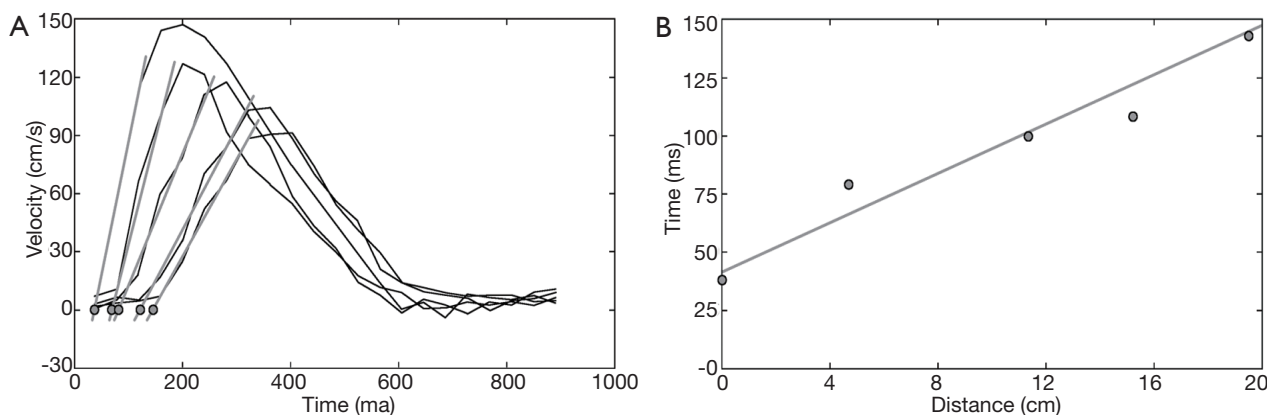
Figure 5 Five velocity waveforms along the length of the aorta (A) each with a linear fit to the upstroke, shown in grey, as well as points identified as the foot of each waveform (grey circles with black borders). The time points associated with the feet of the waveform are plotted against the distance of separation between each plane used to extract the velocity information (B). The slope of a best fit line to the distance versus time plot provides time/distance. The inverse of this slope provides the pulse wave velocity measurement from this series of velocity waveforms.

All of the methods for computing PWV are susceptible to sampling errors and noise. However, depending on the location of the noise—whether pervasive throughout the waveform or solely in the diastolic phase—and how well the waveform happens to be sampled, any one of the TTF, TTU, and XCorr methods can work better than the other. One approach is to use all three methods in the computation of PWV so that the results can be averaged; additionally a result from one of the methods can be rejected should the waveform fail to be amenable to one of the methods. Prior to rejecting data points, it is prudent to inspect the results of the TTF fit, the derivatives for the TTU method, and the correlation plot for the XCorr method to ensure that the algorithm did indeed fail, lest the results of the computations become biased.

MRI-based methods of evaluating pulse wave velocity

As described in the section above, the simplest method to derive PWV from MR data is to determine the temporal shift between the two flow waveforms (28,29,34). The calculation can be performed by acquiring two 2D PC slices and extracting the flow waveforms from each slice (34-36) or more simply by acquiring a single 2D PC slice in the thoracic aorta that transects both the ascending and descending portions of the aorta—thus providing two flow waveforms (37). The use of more than two waveforms (38) potentially decreases the likelihood that sampling error

leads to an erroneous computation of PWV. In fact, Kröner *et al*. demonstrated that the accuracy of PWV measurements improves with more sampling points along the aorta, even at the expense of lower temporal resolution (39). The use of multiple waveforms and therefore multiple slice locations is important in lieu of reflected waves that propagate from the periphery back to the heart; such reflected waves can create abnormalities in flow waveforms that affect PWV measurements. The site of pulse wave reflection varies with age (40), so it cannot be accurately predicted in which slices reflected waves will affect relevant regions of flow waveforms (such as the foot of the waveforms). To use more than two waveforms in the calculation of PWV, the distance between planes is plotted against the time points identified using one of the calculation methods described above (e.g. TTF, XCorr, etc.) (*Figure 5*). A linear line is fitted to the data of this plot. The inverse of the slope of this line is the PWV averaged out over the range of the vasculature covered by the chosen slices. Alternatively, or in addition to this global measurement of PWV, a regional PWV can be computed for each subsequent two slices in the series of 2D PC slices. Such regional PWV measurements are reliable provided that the temporal resolution is sufficient to depict the temporal shift in smaller segments. 2D PC acquisitions generally provide a temporal resolution on the order of 10-30 ms.

Time-resolved 3-dimensional 4D PC MRI with volumetric coverage and velocity sensitivity in all three spatial directions has also been used to compute PWV (*Figure 6*) (41-43). The 4D PC volume of data helps
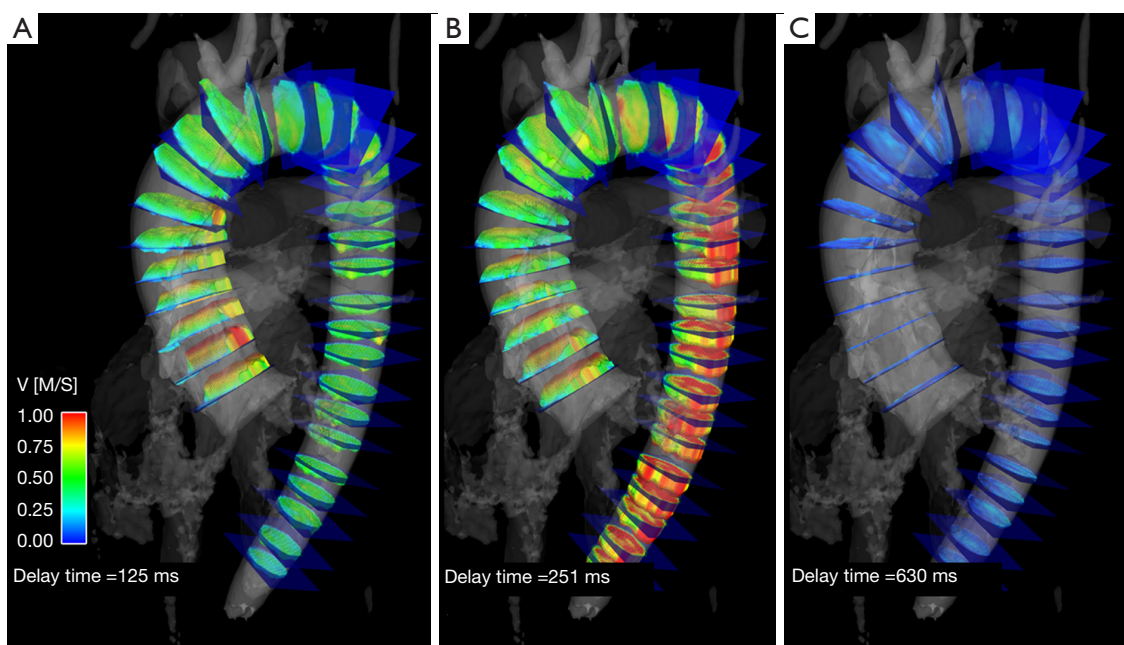
Figure 6 4D phase contrast MRI for the dynamic assessment of pulse wave velocity in a healthy subject shown for 3 out of 20 cardiac phases with delay times from the R-wave of A =125 ms, B =251 ms, and C =630 ms. The anatomical data (grayscale) and the velocity data, shown here as velocity vectors , are all acquired in the same scan and are inherently co-registered. Information on the flow field can be extracted for every location within the image volume. Only selected equidistant planes within the aorta are displayed for improved visibility of the areas of interest. v, velocity (Image provided by Eric Schrauben and Alejandro Roldan, Depts. of Medical Physics and Radiology, University of Wisconsin, Madison, WI, USA).

to overcome patient-specific and/or methodological limitations of 2D PWV measurements, such as potentially tedious and time-consuming slice placement in 2D approaches, particularly in tortuous vessels (*Figure 4B*). However, the achievable temporal resolution is compromised and ranges from 32-50 ms with a scan time of 10-20 minutes (43-45). An advantage of deriving PWV from a 4D volume is that variability in the sampling of the waveforms is mitigated, given both temporal blurring and the fact that all waveforms derived from the volume are gated in synchrony. Furthermore, a 4D PC MRI approach provides the opportunity to derive other hemodynamic parameters of interest from the same scan, including wall shear stress, pressure gradients across stenoses, and other parameters (46).

Fourier velocity encoded (FVE) M-mode imaging is another MR method of deriving PWV. This method uses NMR excitation of a "pencil" beam aligned along a straight segment of a vessel, such as the aorta, to produce M-mode phase contrast images as shown in *Figure 7* (47,48). Data interleaving is employed to increase the effective time

resolution to ~3.5 ms (49,50), which is much better than the temporal resolution obtained with traditional imaging. Simpler 1D projection velocity methods have been proposed that provide a temporal resolution of ~2 ms (51-53). The FVE M-mode acquisition provides a series of images each with a velocity profile along the length of a vessel. A series of images can be reformatted along the time series to provide velocity waveforms for any location along the vessel. These velocity waveforms can be analyzed using the methods above, such as TTF, to provide PWV measurements. The high temporal resolution of this technique allows for both regional and global measurements of PWV. While FVE M-mode imaging provides superior temporal resolution compared to other MR-based methods, the need to image along a straight vessel segment is a limitation, especially because vessels burdened with atherosclerotic disease tend to become tortuous over time (54). Furthermore, atherosclerosis tends to develop at branching points (55), which is problematic for imaging along a straight line, especially in the thoracic aorta.

Westenberg *et al*. have proposed another technique for measuring PWV in which phase contrast slices are
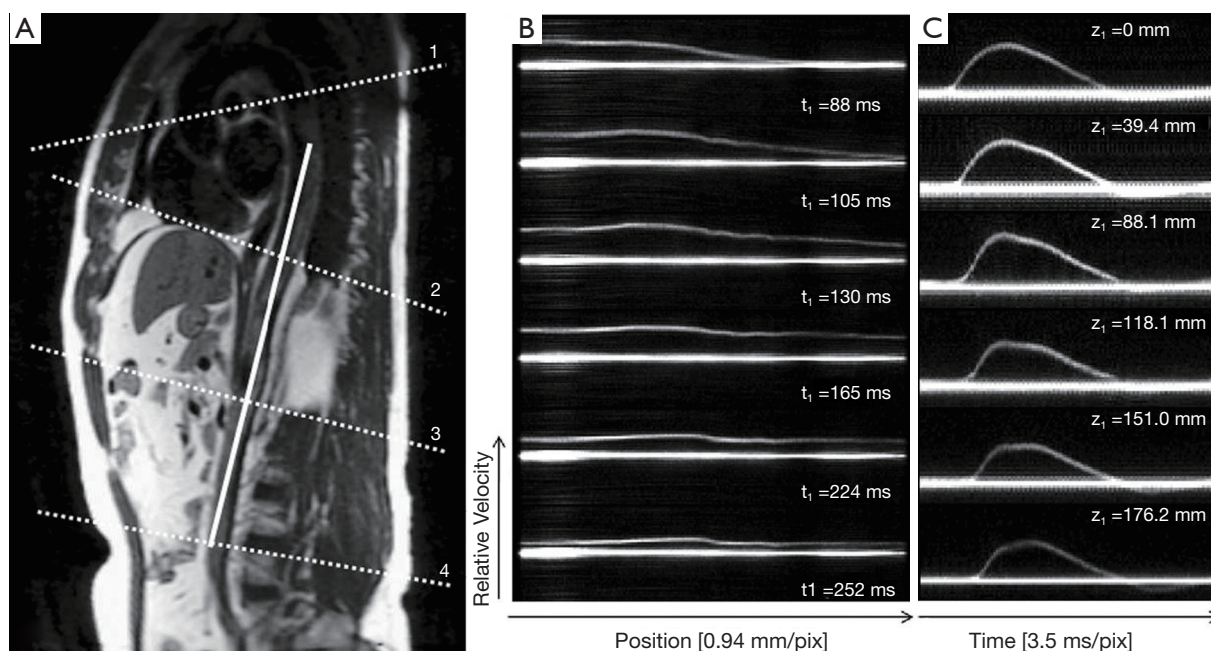
Figure 7 M-mode imaging. (A) A double oblique slice relative to the aorta shows a line through which a pencil beam was applied for M-mode imaging; (B) M-mode images at six different cardiac phases. The straight solid lines represent stationary objects within the pencil beam. The other lines represent blood velocity along the length of the pencil beam at a particular cardiac phase; (C) Reformatted M-mode images along the pencil beam show velocity waveforms over time for a given slice location. Figures reproduced with permission from Taviani *et al*. JMRI 2010 (49). In the original Taviani paper the four slices in (A) identify the slice prescriptions of 2D phase contrast slices. Pulse wave velocity values derived from these slices were compared to pulse wave values computed from M-mode imaging.

acquired double obliquely to the aorta (similar to the view in *Figure 4A*) and are encoded with both anterior-posterior and superior-inferior velocity encoding (39,56). A center line is drawn along the aorta that provides both distance measurements as well as points along which velocity waveforms are derived via the combination of values from the two velocity encoding directions. The acquisition provides an effective temporal resolution of 6-10 ms. This PWV method has the advantage of high temporal resolution with the potential for regional PWV measurements. This method also has greater coverage of the vasculature compared to the FVE M-mode method. It should be noted that the acquisition time is relatively long—up to 14 minutes in duration depending on the subject's heart rate.

It is prudent to briefly discuss the analysis of vessel cross-sectional area as a marker for vascular stiffness (26,57). The principle behind this technique is that the change in vessel area is related to the vessel compliance; compliance is lower in vessels burdened with atherosclerosis. A time-resolved slice orthogonal to a vessel is acquired; the

area of the vessel is measured in both systole and diastole. Compliance, C, is then measured by dividing the change in area, ΔA, by pulse pressure, ΔP, as measured by a sphygmomanometer, such that $C=\Delta A/\Delta P$. This method of measuring arterial stiffness does not require sophisticated software; additionally, highly focal points of the vasculature can be assessed. However, the highly focal nature of this technique can be a disadvantage, because the technique is more subject to sampling error such that the results can either under- or over-estimate disease burden depending on the particular plane of analysis. Furthermore, the technique requires high spatial resolution to accurately assess changes in vessel area. A more thorough discussion of methods for quantifying compliance is discussed by Oliver and Webb (58). Compliance also can be used to derive PWV such that $PWV=\Delta Q/\Delta A$; this is termed the QA method (59-61). PWV is calculated by plotting vessel area versus flow as measured in a time series of a 2D PC slice through a vessel. A best fit line is fitted to the early systolic portion of this plot to calculate slope; the slope is equivalent to PWV. Ibrahim *et al*. showed good agreement between multi-
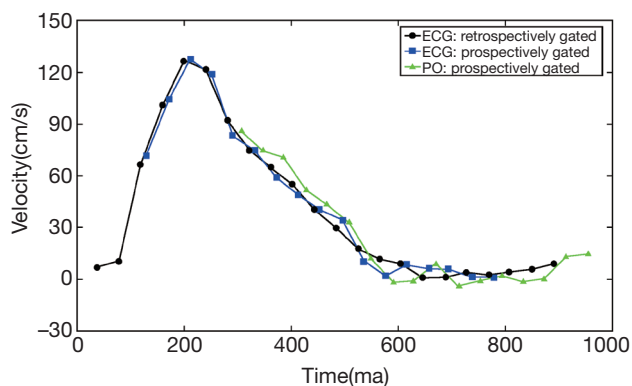
Figure 8 Velocity waveforms in the ascending aorta as acquired with electrocardiogram (ECG) triggering with both prospective and retrospective cardiac gating as well as pulse oximeter (PO) triggering with prospective cardiac gating. Since prospective cardiac gating relies on certain triggers of the ECG/PO waveforms, the acquisition waits for these triggers. For vessels close to the heart, a portion of the velocity waveform has already occurred by the time the trigger has occurred, resulting in missing portions of the velocity waveform. A greater proportion of the waveform is missing with PO triggering because the pulse wave must travel to the finger—leading to a delayed trigger for gating.

slice 2D PC MRI-based PWV measurements and this QA method in the pulmonary arteries (62). However, the processing time for the QA method can be substantial (33).

Prospective versus retrospective cardiac gating

MR-based measurements of PWV rely on acquisitions gated to the cardiac cycle. The gating method employed in acquisitions used for PWV calculations is important, particularly if evaluating PWV with a series of 2D PC slices. Either electrocardiogram (ECG) or peripheral pulse oximeter (PO) gating can be used. For either gating method, the MR acquisition uses prospective or retrospective gating because MRI is too slow to acquire time-resolved images with adequate spatial resolution within a single heartbeat. Retrospective gating often results in prohibitively long scan durations to image within a breath hold, which is desired for imaging in areas subject to respiratory motion (63). Prospective gating can be problematic for PWV measurements, especially when evaluating vessels near the heart or when using the pulse oximeter. The reason for this is that the gating relies on an ECG trigger, such as the QRS complex, to begin the data

acquisition. The detection algorithm for the ECG trigger introduces delays and if slices are acquired near the heart, a portion of the flow wave from early systole may have already passed by the time the data are collected following the QRS complex. As a result, part of the flow waveform is not acquired (*Figure 8*), making it difficult and occasionally impossible to evaluate the waveform with the TTF, TTU and sometimes the XCorr methods.

PO waveforms are usually acquired off a finger, which is more problematic for sampling the entire flow waveforms of vessels near the heart. By the time the pulse wave has traveled to the finger to elicit a change in blood oxygenation, the peak of the pulse wave has traveled well-past the vessels near the heart by the time the data are acquired for the MR acquisition. Thus, an even larger portion of the flow waveform can be missing compared to prospective ECG gating (*Figure 8*).

Alternative methods can be employed to ensure that the entire flow waveform is sampled. As mentioned, retrospective gating methods with Cartesian PC acquisitions can lead to long scan times; respiratory gating or the acceptance of motion artifacts are needed. It has also been shown that retrospective gating with radial PC acquisitions can be used, as this sampling scheme allows for undersampling and the ability to image within the time of a breath hold as well as for flexible retrospective gating since the center of k-space is acquired in every readout (64).

Validation

A number of studies have been performed to validate MR-based measurements of PWV. Suever *et al.* and Rogers *et al.* evaluated multi-slice 2D PC MR-based PWV measurements and compared them to applanation tonometry as a reference standard (65,66). No significant differences were found between the two methods in both patients and controls. Reproducibility of both techniques resulted in a coefficient of variation of ~3.4% for the MR-based PWV measurements and ~6.3% for the applanation tonometry measurements. Multi-slice 2D PC MR-based PWV measurements were also validated against intravascular pressure measurements in 18 patients (67); good agreement was found between methods, with Pearson correlation coefficients ranging from 0.53-0.71. The FVE M-mode method of computing PWV was briefly validated in four human subjects with intravascular pressure probes (50). Again, good agreement between the methods was found with a bias of ~–0.17 m/s

and limits of agreement of –1.55-1.21 m/s for global PWV. Taviani *et al*. further evaluated the accuracy and repeatability of the FVE M-mode method, as well as multi-slice 2D PC MR-based PWV measurements, by imaging a tissue-mimicking phantom with a theoretical PWV as derived from the Moens-Korteweg equation Eq. [1] (49). They determined that the FVE M-mode method was both more accurate and repeatable than the multi-slice 2D PC MR-based method. Bolster *et al*. also did an early study of one-dimensional MR-based PWV measurements versus pressure catheter-based PWV measurements and found good agreement in a phantom (68).

Westenberg *et al*. (56,69) compared both multi-slice one-directional through-plane and in-plane two-directional 2D PC PWV measurements to gold standard intravascular pressure probe PWV measurements in 14-17 patients. These studies demonstrated greater correlation between the in-plane two-directional PWV measurements and the gold standard pressure-based PWV measurements (Pearson correlation coefficient ranging from 0.69-0.91) than between the multi-slice through-plane 2D PC PWV measurements and the gold standard pressure-based PWV measurements.

Outlook

A major limitation to the widespread use of MR-based PWV measurements is the lack of availability of commercial software. A standard software platform is difficult to create given the plethora of MR techniques available, as well as the various algorithms devised for calculating PWV. As researchers gain familiarity with some of the more common PWV techniques, such as presented in this review, developers of commercial flow analysis software packages may begin to incorporate tools for computing PWV.

Additionally, the variety of MR-based PWV methods makes it difficult to choose the most suitable approach. Multi-slice 2D PC PWV measurements are the simplest and the most user-friendly technique, as such sequences are readily available on all scanner platforms. The measurement of PWV from multi-slice 2D PC is also the simplest conceptually and can be readily incorporated into standard flow analysis software. In addition, 2D PC acquisitions provide fairly good temporal resolution (~10-30 ms). Alternatively, FVE M-mode imaging provides the best temporal resolution (~3.5 ms) of the MR-based PWV methods and the greatest ability to perform regional instead of global PWV measurements. However, the necessary

pencil-beam acquisition is not readily available and many researchers and clinicians are generally unfamiliar with the acquisition. The data analysis also is not as simple as multi-slice 2D PC. Two-directional velocity encoding techniques provide the potential for regional PWV measurements and are relatively easy to prescribe. Yet, the acquisition time is long and specialized software is needed to combine the flow waveforms from the two directions and to compute the PWV therefrom. 4D PC methods have the poorest temporal resolution (32-50 ms) of all methods and require the most sophisticated software; they also require a relatively long scan time and currently are not widely available. However, 4D PC techniques hold the potential for an analysis of the vasculature that transcends PWV—providing a one-stop-shop for many flow-related parameters, including PWV, wall shear stress, pressure gradients, flow, turbulent energy, pulsatility index, and more. Nevertheless, much more work is needed to establish these techniques and to make them more widely available.

Acknowledgements

References

1. Strong JP, Malcom GT, McMahan CA, et al. Prevalence and extent of atherosclerosis in adolescents and young adults: implications for prevention from the Pathobiological Determinants of Atherosclerosis in Youth Study. JAMA 1999;281:727-35.
2. Reference Values for Arterial Stiffness' Collaboration. Determinants of pulse wave velocity in healthy people and in the presence of cardiovascular risk factors: 'establishing normal and reference values'. Eur Heart J 2010;31:2338-50.
3. Glagov S, Weisenberg E, Zarins CK, et al. Compensatory enlargement of human atherosclerotic coronary arteries. N Engl J Med 1987;316:1371-5.
4. Voges I, Jerosch-Herold M, Hedderich J, et al. Normal values of aortic dimensions, distensibility, and pulse wave velocity in children and young adults: a cross-sectional study. J Cardiovasc Magn Reson 2012;14:77.

www.thecdt.org   *Cardiovasc Diagn Ther* 2014;4(2):193-206

5. Mohiaddin RH, Longmore DB. MRI studies of atherosclerotic vascular disease: structural evaluation and physiological measurements. Br Med Bull 1989;45:968-90.

6. Kao TW, Taylor HF. High-sensitivity intrinsic fiber-optic Fabry-Perot pressure sensor. Opt Lett 1996;21:615-7.

7. Tabrizchi R, Pugsley MK. Methods of blood flow measurement in the arterial circulatory system. J Pharmacol Toxicol Methods 2000;44:375-84.

8. Nelson MR, Stepanek J, Cevette M, et al. Noninvasive measurement of central vascular pressures with arterial tonometry: clinical revival of the pulse pressure waveform? Mayo Clin Proc 2010;85:460-72.

9. Jiang B, Liu B, McNeill KL, et al. Measurement of pulse wave velocity using pulse wave Doppler ultrasound: comparison with arterial tonometry. Ultrasound Med Biol 2008;34:509-12.

10. Lehmann ED, Parker JR, Hopkins KD, et al. Validation and reproducibility of pressure-corrected aortic distensibility measurements using pulse-wave-velocity Doppler ultrasound. J Biomed Eng 1993;15:221-8.

11. Rajzer MW, Wojciechowska W, Klocek M, et al. Comparison of aortic pulse wave velocity measured by three techniques: Complior, SphygmoCor and Arteriograph. J Hypertens 2008;26:2001-7.

12. Salvi P, Magnani E, Valbusa F, et al. Comparative study of methodologies for pulse wave velocity estimation. J Hum Hypertens 2008;22:669-77.

13. Vermeersch SJ, Rietzschel ER, De Buyzere ML, et al. Distance measurements for the assessment of carotid to femoral pulse wave velocity. J Hypertens 2009;27:2377-85.

14. Huybrechts SA, Devos DG, Vermeersch SJ, et al. Carotid to femoral pulse wave velocity: a comparison of real travelled aortic path lengths determined by MRI and superficial measurements. J Hypertens 2011;29:1577-82.

15. Bossuyt J, Van De Velde S, Azermai M, et al. Noninvasive assessment of carotid-femoral pulse wave velocity: the influence of body side and body contours. J Hypertens 2013;31:946-51.

16. Weber T, Hametner B, Wassertheurer S. Travel distance estimation for carotid femoral pulse wave velocity: is the gold standard a real one? J Hypertens 2011;29:2491; author reply 2491-3.

17. Weber T, Rammer M, Eber B, et al. Determination of travel distance for noninvasive measurement of pulse wave velocity: case closed? Hypertension 2009;54:e137.

18. Joly L, Perret-Guillaume C, Kearney-Schwartz A, et al. Pulse wave velocity assessment by external noninvasive devices and phase-contrast magnetic resonance imaging in the obese. Hypertension 2009;54:421-6.

19. Laurent S, Cockcroft J, Van Bortel L, et al. Expert consensus document on arterial stiffness: methodological issues and clinical applications. Eur Heart J 2006;27:2588-605.

20. Van Bortel LM, Duprez D, Starmans-Kool MJ, et al. Clinical applications of arterial stiffness, Task Force III: recommendations for user procedures. Am J Hypertens 2002;15:445-52.

21. Luo J, Li RX, Konofagou EE. Pulse wave imaging of the human carotid artery: an in vivo feasibility study. IEEE Trans Ultrason Ferroelectr Freq Control 2012;59:174-81.

22. Pignoli P, Tremoli E, Poli A, et al. Intimal plus medial thickness of the arterial wall: a direct measurement with ultrasound imaging. Circulation 1986;74:1399-406.

23. Stein JH, Korcarz CE, Hurst RT, et al. Use of carotid ultrasound to identify subclinical vascular disease and evaluate cardiovascular disease risk: a consensus statement from the American Society of Echocardiography Carotid Intima-Media Thickness Task Force. Endorsed by the Society for Vascular Medicine. J Am Soc Echocardiogr 2008;21:93-111; quiz 189-90.

24. Den Ruijter HM, Peters SA, Anderson TJ, et al. Common carotid intima-media thickness measurements in cardiovascular risk prediction: a meta-analysis. JAMA 2012;308:796-803.

25. Bérard E, Bongard V, Ruidavets JB, et al. Pulse wave velocity, pulse pressure and number of carotid or femoral plaques improve prediction of cardiovascular death in a population at low risk. J Hum Hypertens 2013;27:529-34.

26. Mohiaddin RH, Firmin DN, Longmore DB. Age-related changes of human aortic flow wave velocity measured noninvasively by magnetic resonance imaging. J Appl Physiol (1985) 1993;74:492-7.

27. Yu HY, Peng HH, Wang JL, et al. Quantification of the pulse wave velocity of the descending aorta using axial velocity profiles from phase-contrast magnetic resonance imaging. Magn Reson Med 2006;56:876-83.

28. Boese JM, Bock M, Schoenberg SO, et al. Estimation of aortic compliance using magnetic resonance pulse wave velocity measurement. Phys Med Biol 2000;45:1703-13.

29. Mohiaddin RH. Magnetic resonance imaging of peripheral vascular disease. The state of the artery. Echocardiography 1992;9:553-77.

30. Dogui A, Redheuil A, Lefort M, et al. Measurement of aortic arch pulse wave velocity in cardiovascular MR: comparison of transit time estimators and description of a new approach. J Magn Reson Imaging 2011;33:1321-9.

31. Redheuil A, Yu WC, Wu CO, et al. Reduced ascending aortic strain and distensibility: earliest manifestations of vascular aging in humans. Hypertension 2010;55:319-26.

32. Fielden SW, Fornwalt BK, Jerosch-Herold M, et al. A new method for the determination of aortic pulse wave velocity using cross-correlation on 2D PCMR velocity data. J Magn Reson Imaging 2008;27:1382-7.

33. Ibrahim el-SH, Johnson KR, Miller AB, et al. Measuring aortic pulse wave velocity using high-field cardiovascular magnetic resonance: comparison of techniques. J Cardiovasc Magn Reson 2010;12:26.

34. van der Meer RW, Diamant M, Westenberg JJ, et al. Magnetic resonance assessment of aortic pulse wave velocity, aortic distensibility, and cardiac function in uncomplicated type 2 diabetes mellitus. J Cardiovasc Magn Reson 2007;9:645-51.

35. Leeson CP, Robinson M, Francis JM, et al. Cardiovascular magnetic resonance imaging for non-invasive assessment of vascular function: validation against ultrasound. J Cardiovasc Magn Reson 2006;8:381-7.

36. Laffon E, Marthan R, Montaudon M, et al. Feasibility of aortic pulse pressure and pressure wave velocity MRI measurement in young adults. J Magn Reson Imaging 2005;21:53-8.

37. Shan Y, Lin J, Xu P, et al. Comprehensive assessment of aortic compliance and brachial endothelial function using 3.0-T high-resolution MRI: a feasibility study. J Comput Assist Tomogr 2012;36:437-42.

38. Grotenhuis HB, Ottenkamp J, Fontein D, et al. Aortic elasticity and left ventricular function after arterial switch operation: MR imaging--initial experience. Radiology 2008;249:801-9.

39. Kröner ES, van der Geest RJ, Scholte AJ, et al. Evaluation of sampling density on the accuracy of aortic pulse wave velocity from velocity-encoded MRI in patients with Marfan syndrome. J Magn Reson Imaging 2012;36:1470-6.

40. Sugawara J, Hayashi K, Tanaka H. Distal shift of arterial pressure wave reflection sites with aging. Hypertension 2010;56:920-5.

41. Gu T, Korosec FR, Block WF, et al. PC VIPR: a high-speed 3D phase-contrast method for flow quantification and high-resolution angiography. AJNR Am J Neuroradiol 2005;26:743-9.

42. Markl M, Chan FP, Alley MT, et al. Time-resolved three-dimensional phase-contrast MRI. J Magn Reson Imaging 2003;17:499-506.

43. Wentland AL, Wieben O, François CJ, et al. Aortic pulse wave velocity measurements with undersampled 4D flow-sensitive MRI: comparison with 2D and algorithm determination. J Magn Reson Imaging 2013;37:853-9.

44. Markl M, Wallis W, Brendecke S, et al. Estimation of global aortic pulse wave velocity by flow-sensitive 4D MRI. Magn Reson Med 2010;63:1575-82.

45. Markl M, Wallis W, Strecker C, et al. Analysis of pulse wave velocity in the thoracic aorta by flow-sensitive four-dimensional MRI: reproducibility and correlation with characteristics in patients with aortic atherosclerosis. J Magn Reson Imaging 2012;35:1162-8.

46. Hope MD, Sedlic T, Dyverfeldt P. Cardiothoracic magnetic resonance flow imaging. J Thorac Imaging 2013;28:217-30.

47. Hardy CJ, Bolster BD, McVeigh ER, et al. A one-dimensional velocity technique for NMR measurement of aortic distensibility. Magn Reson Med 1994;31:513-20.

48. Hardy CJ, Bolster BD Jr, McVeigh ER, et al. Pencil excitation with interleaved fourier velocity encoding: NMR measurement of aortic distensibility. Magn Reson Med 1996;35:814-9.

49. Taviani V, Patterson AJ, Graves MJ, et al. Accuracy and repeatability of fourier velocity encoded M-mode and two-dimensional cine phase contrast for pulse wave velocity measurement in the descending aorta. J Magn Reson Imaging 2010;31:1185-94.

50. Taviani V, Hickson SS, Hardy CJ, et al. Age-related changes of regional pulse wave velocity in the descending aorta using Fourier velocity encoded M-mode. Magn Reson Med 2011;65:261-8.

51. Shao X, Fei DY, Kraft KA. Computer-assisted evaluation of aortic stiffness using data acquired via magnetic resonance. Comput Med Imaging Graph 2004;28:353-61.

52. Shao X, Fei DY, Kraft KA. Rapid measurement of pulse wave velocity via multisite flow displacement. Magn Reson Med 2004;52:1351-7.

53. Macgowan CK, Henkelman RM, Wood ML. Pulse-wave velocity measured in one heartbeat using MR tagging. Magn Reson Med 2002;48:115-21.

54. Mochida M, Sakamoto H, Sawada Y, et al. Visceral fat obesity contributes to the tortuosity of the thoracic aorta on chest radiograph in poststroke Japanese patients. Angiology 2006;57:85-91.

55. Nakashima Y, Plump AS, Raines EW, et al. ApoE-deficient mice develop lesions of all phases of atherosclerosis throughout the arterial tree. Arterioscler Thromb 1994;14:133-40.

56. Westenberg JJ, de Roos A, Grotenhuis HB, et al. Improved aortic pulse wave velocity assessment from multislice two-

directional in-plane velocity-encoded magnetic resonance imaging. J Magn Reson Imaging 2010;32:1086-94.

57. Mohiaddin RH, Underwood SR, Bogren HG, et al. Regional aortic compliance studied by magnetic resonance imaging: the effects of age, training, and coronary artery disease. Br Heart J 1989;62:90-6.

58. Oliver JJ, Webb DJ. Noninvasive assessment of arterial stiffness and risk of atherosclerotic events. Arterioscler Thromb Vasc Biol 2003;23:554-66.

59. Vulliémoz S, Stergiopulos N, Meuli R. Estimation of local aortic elastic properties with MRI. Magn Reson Med 2002;47:649-54.

60. Peng HH, Chung HW, Yu HY, et al. Estimation of pulse wave velocity in main pulmonary artery with phase contrast MRI: preliminary investigation. J Magn Reson Imaging 2006;24:1303-10.

61. Herold V, Parczyk M, Mörchel P, et al. In vivo measurement of local aortic pulse-wave velocity in mice with MR microscopy at 17.6 Tesla. Magn Reson Med 2009;61:1293-9.

62. Ibrahim el-SH, Shaffer JM, White RD. Assessment of pulmonary artery stiffness using velocity-encoding magnetic resonance imaging: evaluation of techniques. Magn Reson Imaging 2011;29:966-74.

63. Anderson III AG, Wentland AL, Johnson KM, et al. On the Advantages of Retrospectively Gated Radial

Acquisitions for Cine Phase Contrast Flow Imaging. Proc Intl Soc Mag Reson Med 2011;19:2621.

64. Wentland AL, Korosec FR, Vigen KK, et al. Cine flow measurements using phase contrast with undersampled projections: in vitro validation and preliminary results in vivo. J Magn Reson Imaging 2006;24:945-51.

65. Suever JD, Oshinski J, Rojas-Campos E, et al. Reproducibility of pulse wave velocity measurements with phase contrast magnetic resonance and applanation tonometry. Int J Cardiovasc Imaging 2012;28:1141-6.

66. Rogers WJ, Hu YL, Coast D, et al. Age-associated changes in regional aortic pulse wave velocity. J Am Coll Cardiol 2001;38:1123-9.

67. Grotenhuis HB, Westenberg JJ, Steendijk P, et al. Validation and reproducibility of aortic pulse wave velocity as assessed with velocity-encoded MRI. J Magn Reson Imaging 2009;30:521-6.

68. Bolster BD Jr, Atalar E, Hardy CJ, et al. Accuracy of arterial pulse-wave velocity measurement using MR. J Magn Reson Imaging 1998;8:878-88.

69. Westenberg JJ, van Poelgeest EP, Steendijk P, et al. Bramwell-Hill modeling for local aortic pulse wave velocity estimation: a validation study with velocity-encoded cardiovascular magnetic resonance and invasive pressure assessment. J Cardiovasc Magn Reson 2012;14:2.